STATISTICS, OPTIMIZATION AND INFORMATION COMPUTING
Stat., Optim. Inf. Comput., Vol. **13**, June 2025, pp 2448–2476.
Published online in International Academic Press (www.IAPress.org)

Intelligent Operation of Photovoltaic Generators in Isolated AC Microgrids to Reduce Costs and Improve Operating Conditions

Catalina Díaz-Caceres [1], Luis Fernando Grisales-Noreña [2,*], Brandon Cortés-Caicedo [3], Jhony Andrés Guzmán-Henao [4], Rubén Iván Bolaños [4], Oscar Danilo Montoya-Giraldo [5]

[1] *Department of Electrical Engineering, Faculty of Engineering, Universidad de Talca, Curicó - Chile*
[2] *Grupo de Investigación en Alta Tensión-GRALTA, Universidad del Valle, Cali 760015, Colombia*
[3] *Facultad de Ingeniería, Institución Universitaria Pascual Bravo, Medellín - Colombia*
[4] *Departamento de Mecatrónica y Electromecánica, Facultad de Ingenierías, Instituto Tecnológico Metropolitano, Medellín - Colombia*
[5] *Facultad de Ingeniería, Universidad Distrital Francisco José de Caldas, Bogotá - Colombia*

Abstract This paper addresses the challenges associated with optimizing the operation of photovoltaic distributed generators in isolated electrical microgrids. With the aim of reducing energy production and system maintenance costs and improving the microgrid operating conditions, a master–slave methodology is proposed. In the master stage, the problem of intelligently injecting active power from photovoltaic generators is solved using the continuous versions of four optimization techniques: the Monte Carlo method, the Chu & Beasley genetic algorithm, the population genetic algorithm, and the particle swarm optimizer. Meanwhile, the slave stage evaluates the solutions proposed by the master stage by solving an hourly power flow problem based on the successive approximations method. The proposed solution methodologies are validated in two test scenarios of 10 and 27 buses to select the one with the best performance. Then, the most efficient methodology is implemented in a real isolated grid located in Huatacondo, Chile. This validation aims to assess its ability to optimize the operation of photovoltaic generators in isolated microgrids, considering variations in power generation and demand across the different seasons of the year. The study underscores the importance of financial considerations in achieving an efficient and economically viable operation of photovoltaic generation systems. Furthermore, it provides valuable input to successfully integrate non-conventional renewable energy sources into isolated electrical microgrids.

Keywords Distributed generation, Optimization, Master-slave methodology, Isolated electrical microgrids.

DOI: 10.19139/soic-2310-5070-2247

Nomenclature

AC	Alternating Current
BH	Black Hole optimization
BSS	Battery Storage System
DC	Direct Current
DCCSA	Discrete–Continuous Crow Search Algorithm
DCPPSO	Discrete–Continuous Parallel Particle Swarm Optimization
EMS	Energy Management System

*Correspondence to: Luis Fernando Grisales-Noreña (Email: grisales.luis@correounivalle.edu.co). Grupo de Investigación de Alta Tensión GRALTA, Universidad del Valle, Cali, Colombia (760015).

ISSN 2310-5070 (online) ISSN 2311-004X (print)

ESUSCON	Energía Sustentable Cóndor
GA	Genetic Algorithm
GAMS	General Algebraic Modeling System
MC	Monte Carlo
MINLP	Mixed-Integer Non-Linear Programming
NCRES	Non-Conventional Renewable Energy Sources
NLP	Non-Linear Programming
NPVDG	Number of Photovoltaic Distributed Generators
PA	Periods Analyzed
PGA	Population Genetic Algorithm
PSO	Particle Swarm Optimization
PV	Photovoltaic
PVDG	Photovoltaic Distributed Generators
SMDG	Small Means of Distributed Generation

1. Introduction

Global reliance on fossil fuels for power generation poses significant challenges due to high costs, lack of sustainability, and negative environmental consequences. The transition to renewable and low-carbon energy sources is a pressing need in traditional power systems [28]. In this context, the integration of alternative energies aligned with the requirements of sustainability, economic efficiency, and environmental compatibility becomes a serious and imperative challenge for new generations [24].

Isolated microgrids systems are emerging in response to the need to bring energy to off-grid regions. These systems have traditionally used diesel generators as the primary power source, leading to increased operating costs and emissions of polluting gases [22]. In an effort to follow the energy-efficiency roadmap and harness the solar potential of various regions worldwide, Photovoltaic Distributed Generators (PVDGs) have been integrated into electrical systems. However, even in low-demand and high-generation scenarios, these systems operate at the maximum power point, causing negative effects in terms of voltage profiles, energy losses, and current capacities in the devices that make up the grid [12]. In this sense, an intelligent energy management strategy for PVDGs must ensure compliance with the technical and economic constraints of the isolated microgrids where they are installed. The objective is to avoid power dumping and reductions in energy production—a global problem that is gaining relevance in the operation of electrical distribution systems, particularly in Chile [29]. Addressing this challenge requires mathematically modeling the operation to reduce associated costs, as well as developing efficient strategies to control energy generation and demand.

1.1. Literature review

Various studies on the intelligent operation of solar generation devices in isolated electrical systems have been documented in the specialized literature over the last decade, reflecting a current problem of international interest. Notably, the authors of [4] presented an Energy Management System (EMS) designed for the daily optimization of PVDGs operating in Alternating Current (AC) grids. To this end, the system employed a mathematical formulation based on Non-Linear Programming (NLP) that took into account environmental, financial, and technical aspects as objective functions. The authors proposed a master–slave methodology utilizing the Ant Lion Optimizer (ALO) to determine the energy dispatch of PV sources in one-hour periods within a 24-hour horizon. This methodology was validated in two test scenarios based on urban and rural grids in Colombia. While the results show that this

methodology offers good-quality and repeatable solutions within short processing times, the study lacks a real validation scenario to verify its effectiveness. Moreover, the hourly representation of the system operation in the proposed scenarios may be useful but does not consider the variability in generation capacity due to changing climatic conditions in the region.

The study reported in [19] aimed to explore the application of a parallelized version of the Monte Carlo (MC) method for optimal DG location and operation in isolated AC grids to minimize energy losses during daily operation. The authors used MATLAB and OpenDSS to simulate the major distribution components of the system and perform multiphase calculations. The results displayed short processing times for the solutions obtained with adequate levels of energy loss reduction. However, important aspects, such as the impact of this method on the financial conditions of the grid or the variations in energy demand and production were not considered, limiting the realistic representation of the operation of the systems analyzed. Likewise, the solution methodology was not compared with other approaches proposed in the literature to determine its effectiveness.

In [13], an optimization framework targeting three technical, financial, and environmental objectives was implemented in both rural and urban electricity distribution grids. To this end, the authors employed the Particle Swarm Optimizer (PSO) and the continuous Genetic Algorithm (GA) within a master–slave configuration with an hourly load flow based on the method of successive approximations and considering fluctuations in generation and demand. The first objective function aimed to lower the total energy purchase cost, factoring in the operation and maintenance costs of the PV generation sources. The second objective function sought to reduce the cost associated with energy losses due to the Joule effect in distribution lines. Finally, the third objective function focused on mitigating CO_2 emissions. The authors performed a comparative analysis with several combinatorial optimization methods and evaluated the proposed formulations in 33-bus urban and 27-bus rural test systems to observe the energy performance of Medellín and Capurganá (Colombia), respectively. However, a limitation of the proposed methodology is the absence of a seasonal analysis of energy generation and demand conditions over an extended horizon, as it focuses on a typical day of operation.

The authors of [15] addressed the sizing and location of PV generators within radial distribution grids. Additionally, they used a Mixed-Integer Non-Linear Programming (MINLP) mathematical model to lower annual operating costs over a 20-year timeframe. The objective function integrated energy purchase costs, investment in PV generators, and operating costs. The optimization process involved programming a sine and cosine algorithm in the MATLAB environment to identify optimal locations. Moreover, GAMS software was employed to solve the MINLP model corresponding to the operation of the generators previously located and sized. However, the study only characterized a typical day of operation, which can be a drawback given the proposed 20-year planning horizon. To ensure greater accuracy, it is necessary to account for variations in energy demand and generation conditions, at least during a year-long period. It is also worth noting that the study did not take into account the telescopic characteristics of the system, which might affect operational aspects and limit the current flowing through the lines.

The study presented in [8] explored the optimization of power flow in electrical grids through a combination of metaheuristic and numerical techniques. The authors formulated a MINLP problem to describe this optimization and proposed a master–slave strategy as the solution method. The master stage, on the one hand, used continuous versions of optimization algorithms such as PSO, GA, and BH. The slave stages, on the other hand, employed a method based on successive approximations to compute the objective function, seeking to reduce energy losses during transportation. The methodology was validated using 21-bus and 69-bus test feeders and considering different levels of distributed energy penetration.

Other authors have also proposed optimization models utilizing master–slave methodologies. For example, in [9], a parallelized version of the PSO was employed as part of a master–slave configuration alongside a multi-period power flow method based on successive approximations. The objective was to optimize the operation of Battery Storage Systems (BSSs) in electrical grids with a high penetration of distributed generators. Similarly, the authors of [11] introduced an optimization strategy based on a Discrete–Continuous Parallel Particle Swarm Optimization (DCPPSO) algorithm to efficiently size and locate PV generators. Additionally, in [5], the authors employed a Discrete–Continuous Crow Search Algorithm (DCCSA) to tackle the optimization problem. However, since the study was conducted in a tropical region, the effect of the weather was not assessed, which limited the

results to an average day of operation and diminished their quality. Nonetheless, this simplified scenario served as a reference for selecting the most efficient methodology, which could then be validated in variable generation and demand scenarios across all seasons of the year.

Furthermore, the widespread use of specialized software such as HOMER pro, GAMS, SAM, and CVX for implementing EMSs was discussed in [20]. It should be noted, however, that relying on external applications may limit the functionalities available to network operators, as additional features could entail extra costs.

While all the reviewed studies used existing test systems to confirm the efficiency of their proposed methodologies and focused on a typical 24-hour operation for evaluation, none of them compared the results with real-world scenarios. In addition, they overlooked the variation in energy demand and generation over operating intervals in which the availability of renewable resources may fluctuate. These gaps, however, constitute significant research opportunities in the field.

1.2. Contributions and scope

In line with the studies found in the specialized literature and aiming to address the identified needs, this study proposes a master–slave optimization methodology for the intelligent multi-period operation of PVDGs in isolated microgrids. This approach is intended to lower the costs associated with fossil fuel (diesel) power generation and PVDG maintenance while enhancing the grid operating conditions in terms of power balance, voltage profiles, and loadability of distribution lines.

The master stage, responsible for defining the power dispatch configurations for the PVDGs installed within the isolated microgrid, uses four optimization methods: the Chu & Beasley Genetic Algorithm (CBGA), the Population Genetic Algorithm (PGA), the MC algorithm, and the PSO. Specifically, these algorithms intelligently determine the amount of power to be injected into the grid by each PV generator in hourly periods over a 24-hour horizon. The slave stage, for its part, evaluates each power injection configuration defined by the master stage. To this end, it performs an hourly power flow analysis based on the successive approximation method [14], selected for its effectiveness and reduced convergence times.

The proposed methodology is validated using three test scenarios. The first two scenarios are the 10-bus and 27-bus distribution systems, which are widely discussed in the literature for validating energy management and planning strategies in isolated grids. These systems take into account previously reported generation and demand curves to select the most effective method for problem resolution. On the other hand, the third scenario is a real isolated grid that serves an area in Huatacondo, Chile. This test scenario considers the variations in generation and demand across seasons, sourced from the isolated grid operator, which makes it possible to prove the good performance of the selected methodology under real-world conditions.

This study aims to underscore the importance of financial considerations in achieving an efficient and economically viable operation of PV generation systems in isolated microgrids. In addition, the results contribute to the optimization of PVDG operating costs and performance in isolated microgrids and offer practical solutions for integrating renewable energy sources into electrical systems. This with the purpose of minimizing energy waste and promoting the efficient use of the energy resources available in the region.

The main contributions of this paper to the state of the art are described below:

- A mathematical model for the intelligent management of PV generators in isolated microgrids, which considers operation, generation, and maintenance costs, as well as technical constraints.
- The implementation of four metaheuristic optimization techniques in the master stage that generate power injection configurations for PV generators in varying generation and demand scenarios to lower operating costs and enhance grid conditions.
- The adaptation of a real test system that takes into account the generation, operation, and maintenance constraints under a scenario of variable generation and demand, which is part of an isolated microgrid located in Huatacondo, Chile.
- The selection of the PSO method as the most efficient in terms of quality and repeatability of the solution applied to the problem of managing PVDGs within isolated microgrids. It considers technical and maintenance constraints to minimize operating costs under variable generation and demand scenarios.

1.3. Paper structure

The rest of this paper has been divided into six sections. Section 2 presents the mathematical formulation of the problem of intelligent operation of PVDGs in isolated AC microgrids. Section 3 describes the proposed methodology, which details the adaptation function, the problem coding, each of the optimization techniques employed in the master stage, and the power flow method used in the slave stage. Section 4 introduces each of the test systems used to validate the proposed methodology. Section 5 presents the numerical and graphical analysis of the results. Finally, the conclusions and areas for further research are discussed in Section 6.

2. Mathematical model

This section presents the mathematical formulation to deal with the problem of operating PVDGs in isolated microgrids to lower operating costs and improve operating conditions [7].

2.1. Objective function

The objective function proposed in this paper aims to reduce the microgrid operating costs derived from both energy production by diesel generators and maintenance of PVDGs. This function assumes that the PVDGs are either owned by the grid operator or the microgrid owner; therefore, the energy costs associated with these generators are equal to zero.This assumption simplifies the optimization model. In such cases, the generation costs of solar energy are considered negligible because PVDGs have no variable fuel costs, unlike fossil fuel-based technologies. By assuming zero energy costs, the focus shifts to efficiently managing available resources and optimizing the interaction between the microgrid and the main grid. It is worth highlighting that this paper focuses on a 24-hour operational horizon and that the proposed formulation considers only active energy management, as this scenario is widely analyzed in the specialized literature. The objective function of the system is represented by Equation (1):

$$\min E_{\cos t} = C_{kWh}\left(\sum_{h\in\mathcal{H}}\sum_{i\in\mathcal{N}} P^{gc}_{i,h}\Delta h\right) \quad + C_{O\&M}\left(\sum_{h\in\mathcal{H}}\sum_{i\in\mathcal{N}} P^{pv}_{i,h}\Delta h\right) \tag{1}$$

Where $p^{gc}_{i,h}$ is the active power supplied by each conventional generator and $p^{pv}_{i,h}$ is the active power injected by each PVDG connected to node i in time period h. The term $\mathcal{N}$ represents the set of nodes comprising the grid and $\mathcal{H}$ refers to all the periods in the analyzed time horizon. The notation Δh indicates the duration of each period, which, in this study, is defined as one hour. Finally, C_{kWh} and $C_{O\&M}$ denote the energy cost per kWh and the operation and maintenance cost of each PVDG, respectively. The value of $C_{O\&M}$ is reported as USD 0.0019 in [32], whereas C_{kWh} varies depending on the electrical system. For the 10-bus and 27-bus systems, C_{kWh} is reported as USD 0.2913 in [13], whereas for the Huatacondo system, it is reported as USD 0.3249.

To determine the energy production cost for the Huatacondo system, the following analysis is conducted: The cost of diesel in the city of Pozo Almonte is CLP 1,045 [3]. Additionally, the technical specifications of the Cummins Diesel PE-120CD electric generator indicate a consumption rate of 26 lt/h and a power output of 96 kW. These data are utilized to calculate the cost of energy generation per hour in Chilean pesos.

$$C^{Huatacondo}_{kWh} = 26\text{lt/h} \cdot 1045\text{CLP/lt} = 27170\text{CLP/h} \tag{2}$$

Using the generator power data, we obtain the cost of energy production for the diesel generator per kWh.

$$C^{Huatacondo}_{kWh} = 27170\,\text{CLP/h} \div 96\,\text{kWh/h} = 283,0208\,\text{CLP/kWh} \tag{3}$$

$$C^{Huatacondo}_{kWh} = 283,0208\,\text{CLP/kWh} \div 871\,\text{CLP/USD} = 0,3249\,\text{USD/kWh} \tag{4}$$

2.2. *Constraints*

Operating constraints refer to equations, limits, and parameters that model the system's behavior. The solution to the intelligent PVDG operation and hourly power flow problem must satisfy this set of constraints to ensure the system's safe and efficient operation. Initially, the balance equations for the power supplied and consumed in the grid are established. Equation (5) expresses the active power balance, where $P^{gc}_{i,h}$ is the active power supplied by the conventional generator, $P^{d}_{i,h}$ is the active power demanded by the loads, and $P^{pv}_{i,h}$ is the active power supplied by the PVDGs at node i for each period h. Meanwhile, Equation (6) illustrates the reactive power balance, where $Q^{gc}_{i,h}$ is the reactive power supplied by the conventional generator and $Q^{d}_{i,h}$ is the reactive power demanded at node i for each period h.

$$p^{gc}_{i,h} + p^{pv}_{i,h} - P^{d}_{i,h} = v_{i,h} \sum_{j \in \mathcal{N}} Y_{ij} v_{j,h} \cos\left(\theta_{i,h} - \theta_{j,h} - \varphi_{ij}\right), \left\{\forall i \in \mathcal{N}, \forall h \in \mathcal{H}\right\} \tag{5}$$

$$q^{gc}_{i,h} - Q^{d}_{i,h} = v_{i,h} \sum_{j \in \mathcal{N}} Y_{ij} v_{j,h} \sin\left(\theta_{i,h} - \theta_{j,h} - \varphi_{ij}\right), \left\{\forall i \in \mathcal{N}, \forall h \in \mathcal{H}\right\} \tag{6}$$

The operating limits that ensure the safe and efficient operation of the conventional generator are expressed by the following equations:

$$P^{gc,\min}_{i} \leq P^{gc}_{i,h} \leq P^{gc,\max}_{i}, \left\{\forall i \in \mathcal{N}, \quad \forall h \in \mathcal{H}\right\} \tag{7}$$

$$Q^{gc,\min}_{i} \leq Q^{gc}_{i,h} \leq Q^{gc,\max}_{i}, \left\{\forall i \in \mathcal{N}, \quad \forall h \in \mathcal{H}\right\} \tag{8}$$

Equation (7) denotes the active power limits of the conventional generator (G), where $P^{gc,\min}_{i}$ and $P^{gc,\max}_{i}$ are the minimum and maximum power supplied, respectively. For its part, Equation (8) expresses the reactive power limits, where $Q^{gc,\min}_{i}$ and $Q^{gc,\max}_{i}$ are the minimum and maximum power supplied.

The power that a panel can deliver is directly linked to its electrical characteristics and the environmental conditions in which it operates. Therefore, the following equations model the panel's behavior, considering its power constraints:

$$P^{pv,\min}_{i} \leq P^{pv}_{i} \leq P^{pv,\max}_{i}, \left\{\forall k \in \mathcal{N}\right\} \tag{9}$$

$$P^{pv,\min}_{i} \leq P^{pv}_{i,h} \leq P^{pv}_{i} G^{pv}_{h}, \left\{\forall i \in \mathcal{N}, \quad \forall h \in \mathcal{H}\right\} \tag{10}$$

Equation (9) represents the active power range that the panel can deliver, where $P^{pv,\min}_{i}$ and $P^{pv,\max}_{i}$ are the limits. The maximum limit is reached when the PVDGs operate at the maximum power point during an average day of operation. Equation (10) indicates that the maximum power that the panel can deliver is determined by the typical generation curve of the region in which it is located. In addition, its generation behavior, denoted by G^{pv}_{h}, depends on aspects such as radiation, temperature, and technology type. It should be noted that, in this study, the reactive component of the PV panels is neglected [5]. Lastly, Equation (11) presents the minimum $V^{\min}_{i}$ and maximum $V^{\max}_{i}$ voltage variation limits allowed at each node of the system. Meanwhile, Equation (12) shows that the line current between nodes i and j in each period h, denoted by $i_{ij,h}$, must not exceed the maximum current $I^{\max}_{ij}$ supported by each grid section.

$$V^{\min}_{i} \leq v_{i,h} \leq V^{\max}_{i}, \left\{\forall i \in \mathcal{N}, \quad \forall h \in \mathcal{H}\right\} \tag{11}$$

$$|i_{ij,h}| \leq I^{\max}_{ij}, \left\{\forall i, j \in \mathcal{N}, \quad \forall h \in \mathcal{H}\right\} \tag{12}$$

3. Solution methodology

This section describes the proposed solution methodologies for assessing the intelligent operation of PVDGs within isolated microgrids, aimed at reducing the costs derived from maintaining PVDGs and purchasing energy from conventional generators.

Optimally operating PVDGs in electrical systems is considered to be a non-linear and non-convex problem [30]. Consequently, this study employs numerical methods and metaheuristic optimization algorithms to solve it. Metaheuristic algorithms have been chosen for their simplicity and high efficiency in addressing energy management challenges in electrical grids [1, 5]. To this end, a master–slave methodology is adopted, where the problem is divided into two stages: The initial or master stage implements an optimization method to ascertain the ideal level of power to be injected by the PVDGs. Subsequently, the second or slave stage leverages a numerical method to assess the solutions achieved in the master stage according to a defined fitness function.

3.1. Adaptation function

To ensure compliance with the technical operating constraints, specifically the voltage constraints at each node (Equation (11)) and the current constraints for each line (Equation (12)), we propose the adaptation function. This function refers to the objective function value plus a penalty value, which is applied in response to potential violations of voltage or current constraints. It is important to highlight that the verification of potential violations is carried out through the proposed slave stage, which employs a power flow method for each time period. In this study, we use a power flow analysis applying the successive approximations method. These constraints encompass both voltage regulation (±8%) and line loadability (exceeding 100%), ensuring that the operating constraints of the problem addressed in this study are considered. The adaptation function utilized in this study is presented in Equation (13).

$$fadap = FO + \alpha Pen_V + \beta Pen_I \tag{13}$$

$$Pen_V = \sum_{i\in\mathcal{N}}\sum_{h\in\mathcal{H}} \max(0, v_{i,h} - V_i^{\max}) - \min(0, v_{i,h} - V_i^{\min}) \tag{14}$$

$$Pen_I = \sum_{i\in\mathcal{N}}\sum_{j\in\mathcal{N}}\sum_{h\in\mathcal{H}} \max(0, i_{ij,h} - I_{ij,h}^{\max}) \tag{15}$$

Where FO represents the objective function shown in Equation (1). Pen_V and Pen_I denote the penalties for voltage regulation and line loadability violations, respectively. For their part, α and β are the penalty factors strategically designed to influence the magnitude of the penalty associated with potential violations of the system's operating constraints. These factors are chosen heuristically with a value of 1000. For computing Pen_V, the voltage violations recorded at all nodes during the 24 hours of operation are summed using Equation (14). Moreover, Equation (15) is employed to include the penalties for violations of the line loadability. The remaining constraints are ensured through power balance and the proposed coding, thereby avoiding the generation of additional penalties that could increase the convergence times of the algorithms.

3.2. Proposed coding

The problem at hand is represented by a vector coding of size $[1, H \times |PVDG|]$, where H denotes the number of periods within the analyzed time horizon, specifically 24 periods in an average operating day. For its part, $|PVDG|$ represents the number of PVDGs within the grid. As illustrated in Figure 1, a power level to be dispatched in each time period is proposed for each generator. This value is limited by the maximum and minimum values obtained in the power curve of each generator operating at the maximum power point.

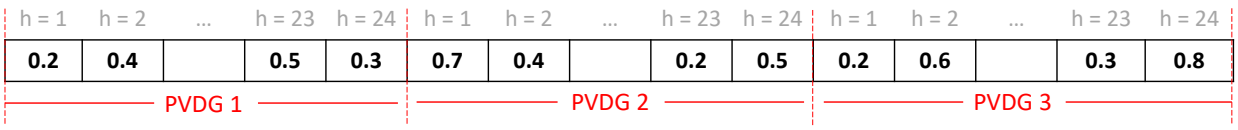

Figure 1. Coding for the operation of photovoltaic distributed generators.

3.3. Master stage

This stage proposes various PVDG dispatch configurations to explore the solution space by applying evolutionary criteria based on population algorithms. Four optimization techniques are implemented in this stage: the Monte Carlo optimization method, continuous versions of the Chu & Beasley genetic algorithm and the population genetic algorithm, and the particle swarm optimizer. These methods were chosen for their exceptional performance in overcoming analogous challenges within the realm of electrical engineering.

3.3.1. Monte Carlo optimization method MC is an optimization technique renowned for its ability to assess numerous randomly proposed scenarios, thereby finding a high-quality solution within a predefined number of iterations [10]. This straightforward method generates a population of individuals in every iteration, with each individual constituting a potential solution to the problem at hand. Subsequently, the objective function is evaluated for each individual, ensuring adherence to the problem constraints. The top solution from each iteration is put on an elite list. Finally, when the iterative process is completed, the optimal solution is selected from that elite list [19].

In this study, each individual represents the hourly power injection of the PVDGs installed in the system. The step-by-step MC method followed in this paper is described below:

1. Initialization. The system data and the power limits of the PVDGs are loaded. Algorithm parameters such as the number of iterations and individuals are also defined.
2. Generation of random solutions. Random solutions are generated within the previously defined power range, ensuring that they are different from each other. As many random solutions are generated as there are individuals in the population.
3. Evaluation of the adaptation function. The adaptation function that represents the problem is evaluated for every individual in the population within the slave stage.
4. Compilation of the elite list. The top solution among the generated population of individuals is selected and put on the elite list.
5. Convergence. The process is run again from step 2 until reaching the previously defined maximum limit of iterations.
6. Best solution. Upon reaching the convergence criterion, the elite list is evaluated and the optimal result is selected as the solution to the problem.

3.3.2. Chu & Beasley genetic algorithm The GA is inspired by the mechanism of natural selection, a biological process in which the strongest individuals are more likely to succeed in a competitive environment [18]. The method consists of three essential processes: generating the initial population, implementing genetic operators to obtain a single descendant (selection, crossover, and mutation), and assessing the convergence or stopping criteria of the algorithm [8]. The selection, crossover, and mutation criteria that govern the exploration of the CBGA are described below [23]:

- **Selection.** The offspring population selects the fittest chromosomes from the current population to serve as parents for the next generation. This selection process involves randomly choosing four parents and playing a tournament where they are compared according to the value of their adaptation function. The pair of parents with the lowest fitness function is then selected to produce offspring.
- **Crossover.** This process alters the offspring population by applying an operator that combines characteristics from different chromosomes to generate new solutions. Since this problem operates with continuous variables, this study takes the average of the values within the two individuals selected as parents to generate offspring.
- **Mutation.** Random mutations of certain genes in the selected chromosomes are introduced. This causes variability in the population and expands the space of evaluated solutions, preventing premature convergence to a suboptimal solution. In this study, the offspring has some characteristics mutated within the minimum and maximum power values set for each time period.

The main steps of the CBGA are explained below:

1. Initialization. The system data and the power limits of the PVDGs are loaded. Algorithm parameters such as the number of chromosomes or individuals, the number of generational cycles or iterations, and the number of mutations are also defined.
2. Initial population. The original population of individuals, also known as chromosomes, is generated. Each chromosome contains genes that encode the values of the decision variables. In this study, a random value between the minimum and maximum power is generated in the PVDGs for each time period. The power limit for each time period is obtained by operating the PVDG at the maximum power point.
3. Evaluation of the adaptation function. The adaptation function that represents the problem is evaluated for every individual in the population within the slave stage.
4. Generation of the offspring. Using the selection, crossover, and mutation operators, a descendant is generated for the problem, i.e., a power dispatch scheme for the PVDGs installed within the microgrid.
5. Evaluation of the adaptation function of the offspring. The adaptation function of the offspring is evaluated in the slave stage.
6. Replacement of the worst parent and update of the incumbent. If the offspring outperforms its parent in terms of the adaptation function, it replaces the parent within the population. Therefore, the problem incumbent is modified.
7. Convergence. The process is run again from step 4 until the convergence criterion is met, which is reaching the maximum limit of iterations.

3.3.3. Population genetic algorithm The PGA is utilized to solve complex optimization problems. It differs from the previous method mainly in the way the population is handled. While the CBGA modifies one individual at each iteration, the PGA modifies the entire population, allowing for greater diversity and exploration of the solution space. The algorithm's population characteristic determines the number of descendants, denoted by N, to form the new population. The offspring could either replace the parent generation or mix with them in the next generation, following the principles of biological evolution, where the "strongest" organism prevails.

This algorithm employs the same selection, crossover, and mutation principles as the CBGA. The steps for implementing the algorithm are detailed below:

1. Initialization. The system data and the power limits of the PVDGs are loaded. Algorithm parameters, including the number of chromosomes, generational cycles, mutations, and offspring to be generated in the new population, are also defined.
2. Initial population. The original population of individuals is generated. As in the CBGA, the chromosomes contain the values of the decision variables, i.e., they represent a power value injected by the PVDGs within the established range.
3. Evaluation of the adaptation function. The adaptation function that represents the problem is evaluated for each individual in the population within the slave stage. The population is then organized into a matrix based on its adaptation function.
4. Generation of the offspring. Using the selection, crossover, and mutation operators on the parent population, a portion of the descendant population is generated (intensification). The remaining portion is created randomly to broaden the solution space (diversification).
5. Evaluation of the adaptation function of the offspring. The adaptation function of the offspring is evaluated in the slave stage.
6. Sorting and selection of the new population. The total solution population, comprising the parent population and the newly generated offspring, is sorted according to its adaptation function. This ensures that individuals achieving the best results are selected to form the new population.
7. Convergence. The process is run again from step 4 until the convergence criterion is met, which is reaching the maximum limit of iterations.

3.3.4. Particle swarm optimizer The PSO is a methodology for optimizing non-linear functions inspired by social and cognitive behavior. It simulates the movement of particles through hyperspace, with each particle representing

a probable solution to the optimization issue [16]. With every iteration, the algorithm aims to stochastically improve these solutions by adjusting their velocities based on the best position of each particle (p_{Best}) and the best known position of the entire swarm (g_{Best}) [31]. In this study, the position indicates the amount of power injected by the PVDGs, while the velocity represents the delta that makes the power vary at each iteration. In addition, the population size is determined by the number of PVDGs in the system and the hours of power injection [23].

The steps to implement the PSO through code are outlined below:

1. Initialization. The system data and the power limits of the PVDGs are loaded. Algorithm parameters, including the number of particles, velocity and inertia limits, cognitive and social factors, and the number of maximum iterations are also defined. Moreover, the initial position and velocity of each particle are randomly generated.
2. Evaluation of the adaptation function of the initial population. The adaptation function is evaluated at the current position of each particle. Also, for each particle, the best local solution (p_i) is set, which is equal to its current position. Moreover, the best global solution (P_g) is established, which is equal to the solution within the swarm that achieved the best adaptation function value.
3. From the second iteration, Equation (16), which governs the velocity behavior of each particle, is used to displace the particles within the solution space.

$$v_{ij}^{t+1} = w \cdot v_{ij}^{t} + c_1 \cdot r_1 \cdot (p_{ij}^{t} - x_{ij}^{t}) + c_2 \cdot r_2 \cdot (p_{gj}^{t} - x_{ij}^{t}) \tag{16}$$

   Where v_{ij}^{t+1} is the velocity reached by particle i in dimension j at time $t+1$. w denotes the inertia factor, which regulates the influence of the prior velocity on the updated velocity. v_{ij}^{t} signifies the velocity attained by particle i in dimension j at time t. c_1 and c_2 are constant acceleration coefficients. r_1 and r_2 are random numbers uniformly distributed in the interval [0,1]. p_{ij}^{t} denotes the most favorable position of particle i in dimension j at time t. x_{ij}^{t} represents the position of particle i in dimension j at time t. Lastly, p_{gj}^{t} is the optimal swarm position in dimension j at time t.
4. Update of the position. The position of the particle is updated using Equation (17).

$$x_{ij}^{t+1} = x_{ij}^{t} + v_{ij}^{t+1} \tag{17}$$

5. Evaluation of the adaptation function. The adaptation function that represents the problem is evaluated for each particle in the swarm at their new position within the slave stage.
6. Update of the best local and global positions. Based on the adaptation function values obtained by the particle swarm, the values of (p_i^t) and (P_g^t) are updated in each iteration.
7. Convergence. The process is run again from step 3, adjusting the velocity and position values, until the convergence criterion is met, which is reaching the maximum limit of iterations.

3.4. Slave stage

To assess the impact on energy production costs and address technical constraints related to line loadability and node voltage regulation, it is essential to ascertain the power flow for the different time periods defined. In this study, an hourly power flow analysis was performed applying successive approximations. This method was chosen due to its reported benefits, including reduced processing times and fast convergence to the solution [5].

The successive approximation method employed for dealing with power flow in electrical systems was first introduced by Montoya et al. in [21]. The steps for implementing this method are explained below:

1. Initialization. The system data and parameters such as the PVDG location nodes, the demanded power, the current limits, the PVDG power determined by the master stage, the maximum limit of iterations, and the convergence error are loaded. Moreover, the cost factors associated with energy production and panel maintenance are also input.
2. Computation of electrical parameters. The system admittance matrix is computed using the grid data.
3. Evaluation. The node voltages are established for each hour of operation at the demand nodes (d) only; at the generation nodes (slack), these values are already known. For this purpose, the power flow is computed hour

by hour using the following recursive equation:

$$V_{d,h}^{t+1} = -Y_{dd}^{-1}[diag^{-1}(V_{d,h}^{t,*})(S_{d,h}^{t,*} - S_{pv,h}^{*}) + Y_{ds}V_{s,h}] \tag{18}$$

Where t represents the iteration counter. $V_{d,h}$ denotes the vector that indicates the voltage at the demand nodes for each time period h. Y_{ds} is the admittance matrix section linking the slack node with the demand nodes, while Y_{dd} is the admittance matrix section relating the demand nodes to each other. $S_{d,h}$ signifies the complex domain vector encompassing the reactive and active power demanded at the load nodes for each time period h. $S_{pv,h}$ is the complex domain vector containing the active power that each PVDG produced for each time period h. Lastly, $V_{s,h}$ represents the vector that contains the voltage at the substation node terminals for each time period h, which serves as a known parameter within the power flow solution. In this context, the asterisk symbol $(*)$ denotes the conjugate of the complex number.

4. Power flow solution and convergence. Equation (18) is solved iteratively until the convergence criterion is met. Equation (19) represents the convergence criterion, where ϵ is the error parameter defined in this paper as $1 \cdot 10^{-10}$. A flat voltage at all nodes of the system (1 p.u.) serves as the starting point for the calculation.

$$\left| V_{d,h}^{t+1} - V_{d,h}^{t} \right| \leq \epsilon \tag{19}$$

5. Evaluation of the adaptation function. Once the voltage levels associated with each hour of operation have been calculated, the adaptation function for each hour is evaluated using Equation (13). This adaptation function consists of the objective function (focused on minimizing energy production and PVDG maintenance costs) and the penalties linked to the loadability and voltage regulation constraints.
6. Return of the adaptation function to the master stage. After computing the adaptation function for each hour of operation, the results obtained across all hours are summed and returned to the master stage.

4. Test systems

This section describes the topologies and electrical parameters of the three test feeders used in this paper. We begin with the 10-bus and 27-bus systems, which are extensively implemented in the literature to validate energy planning and management strategies [5, 13]. Our analysis is performed in Colombia, where generation and demand conditions are similar throughout the year due to the geographical features of the region. Subsequently, we focus on ESUSCON, a real isolated microgrid located in the Tarapacá region in Chile, which considers the varying generation and demand conditions across seasons. Its parameters and components are also characterized in this section.

For the 10-bus and 27-bus feeders, we adapted the rural demand and generation curves reported in the literature for Capurganá, Colombia [13]. To characterize these curves, we used ambient temperature and solar radiation data sourced from the National Aeronautics and Space Administration (NASA) database [33]. These data, spanning from January 1 to December 31, 2019, and recorded at one-hour intervals, are listed in Table 1. Based on these data and the parameters of a polycrystalline silicon panel, we obtained the behavior curve (p.u.) for this panel type in the region under analysis. To derive this curve, we employed the equations proposed in [13], as shown in the last column of Table 1.

Figure 2 below illustrates the anticipated power generation (in p.u.) from a solar panel in Capurganá, Colombia. This profile will help us validate the optimization methodologies in the two test systems that are here being examined.

To determine the energy demand curve for Capurganá's isolated electrical grid, we analyzed consumption data from historical records provided by IPSE [27]—the entity in charge of overseeing the non-interconnected areas in Colombia. Such consumption data are presented at one-hour intervals in Table 2. Using this data, we constructed the energy demand curve for Capurganá's isolated grid, as shown in Figure 3. This curve represents energy demand on a typical day of operation for the same time period analyzed in solar generation. Using profiles from a typical day allows the evaluation of system performance under representative operating conditions. These profiles are

Table 1. Daily average solar power generation in Capurganá (Colombia) [13].

Hour	G_T **[W/m2]**	T_a **[°C]**	C_{pu} **[p.u.]**
1	0	24.44252	0
2	0	24.32474	0
3	0	24.22545	0
4	0	24.14674	0
5	0	24.08422	0
6	0	24.03482	0
7	29.14570	24.10367	0.02770
8	142.11066	24.78126	0.13277
9	291.61926	25.68211	0.26622
10	431.95384	26.63671	0.38547
11	540.61581	27.47515	0.47362
12	605.16362	28.10252	0.52397
13	606.93027	28.46775	0.52442
14	583.07479	28.56923	0.50519
15	490.55904	28.42334	0.43065
16	359.22033	28.03460	0.32148
17	204.48775	27.44945	0.18722
18	64.51775	26.69008	0.06034
19	3.17460	25.89016	0.00300
20	0	25.39227	0
21	0	25.09285	0
22	0	24.87663	0
23	0	24.70841	0
24	0	24.56926	0

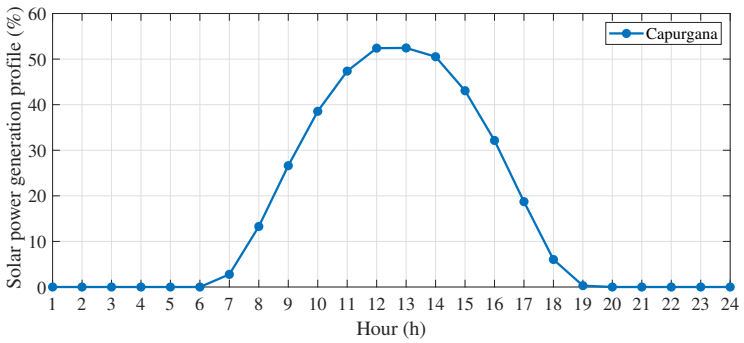

Figure 2. Anticipated solar power generation in Capurganá (Colombia) [13].

based on real data, ensuring realism in the model. Although seasonal variations are not initially considered, this approach simplifies the analysis and helps assess the feasibility of photovoltaic integration without introducing the complexity of long-term scenarios.

4.1. 10-bus test feeder

The 10-bus test feeder documented in the existing literature is depicted in Figure 4 [30]. Ten buses and nine lines comprise this radial distribution system, which runs at a power and base voltage of 100 kVA and 23 kV, respectively.

Table 2. Average energy demand in Capurganá (Colombia) [13].

Hour	P_d **[kW]**	P_d **[p.u.]**
1	428.04117	0.84573
2	409.76717	0.80962
3	317.81654	0.62795
4	256.70648	0.50720
5	51.70864	0.10217
6	11.05835	0.02185
7	32.49553	0.06421
8	62.77491	0.12403
9	119.17381	0.23547
10	281.26057	0.55572
11	333.09429	0.65813
12	358.36076	0.70805
13	368.01140	0.72712
14	369.70917	0.73048
15	379.97901	0.75077
16	388.65478	0.76791
17	386.78365	0.76421
18	395.19266	0.78083
19	430.88177	0.85134
20	464.61670	0.91800
21	476.40313	0.94128
22	473.67462	0.93589
23	467.29281	0.92328
24	452.18590	0.89344

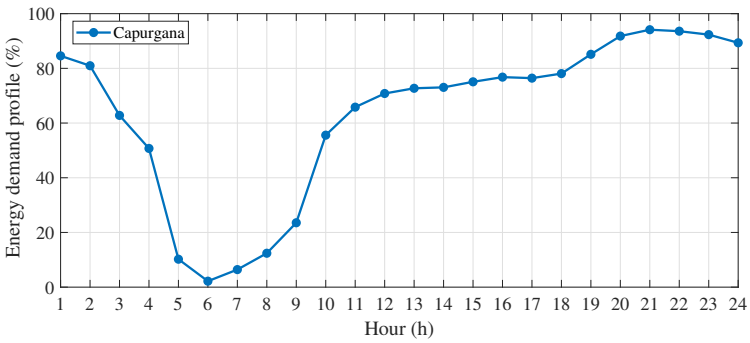

Figure 3. Anticipated energy consumption in Capurganá (Colombia) [13].

As observed, this grid incorporates three PV generators situated at buses 5, 9, and 10, each with a nominal power of 2,400 kW. Limiting the study to three PVDGs strikes a balance between computational complexity and system representativeness. This number reflects typical microgrid configurations with a moderate number of PVDGs. It allows for the assessment of both individual and collective impacts of the generators on microgrid operation without compromising the computational feasibility of the model.

Table 3 presents the parameters for the lines within the system, encompassing the line identifier, sending node (i), receiving node (j), and resistance (R_{ij}) and reactance (X_{ij}) of the line between nodes i and j. Additionally, it includes the active (P_j) and reactive power (Q_j) requirements at the receiving node, along with the maximum

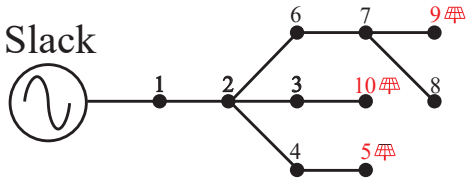

Figure 4. Radial topology of the 10-bus test feeder.

permissible current (I_{max}). It is crucial to emphasize that this test system's lines are considered telescopic in this study, meaning that both their diameter and the conductors' maximum current carrying capacity decrease as they get farther from the substation bus [4]. The lines' maximum current capacity was here determined by computing an hourly power flow within the system, assuming that there were no PVDGs and setting current thresholds based on Form No. 4 of the PMGD PFV Nan project issued by the CGE [2].

Table 3. Electrical parameters for the 10-bus test feeder.

Line	**Node** i	**Node** j	R_{ij} (Ω)	X_{ij} (Ω)	P_j **[kW]**	Q_j **[kVAr]**	I_{max} **[A]**
1	1	2	0.1233	0.4127	1840	460	550
2	2	3	0.2467	0.6051	980	340	150
3	2	4	0.7469	1.2050	1790	446	195
4	4	5	0.6984	0.6084	1598	1840	114
5	2	6	1.9837	1.7276	1610	600	195
6	6	7	0.9057	0.7886	780	110	150
7	7	8	2.0552	1.1640	1150	60	99
8	7	9	4.7953	2.7160	980	130	99
9	3	10	5.3434	3.0264	1640	200	99

4.2. 27-bus test feeder

The arrangement of the lines and buses in the 27-bus test feeder is shown in Figure 5. This radial distribution system comprises 27 buses and 26 lines, with a power and a base voltage of 100 kVA and 23 kV, respectively. Importantly, this configuration incorporates three PV generators positioned at buses 5, 9, and 19, each rated at 2,400 kW. A full description of this test feeder is provided in [13].

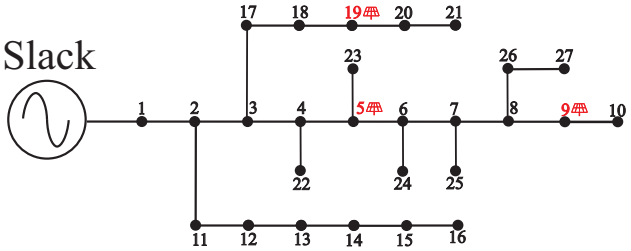

Figure 5. Radial topology of the 27-bus test feeder.

The parameters for the lines within this system are presented in Table 4 using the same format employed in Table 3. In this test system, the distribution lines are considered telescopic, and the data regarding maximum current carrying capacity was taken from [13].

Table 4. Electrical parameters for the 27-bus test feeder.

Line	**Node** i	**Node** j	R_{ij} (Ω)	X_{ij} (Ω)	P_j **[kW]**	Q_j **[kVAr]**	I_{max} **[A]**
1	1	2	0.0140	0.6051	0	0	240
2	2	3	0.7463	1.0783	0	0	165
3	3	4	0.4052	0.5855	297.50	184.37	95
4	4	5	1.1524	1.6650	0	0	85
5	5	6	0.5261	0.7601	255.00	158.03	70
6	6	7	0.7127	1.0296	0	0	55
7	7	8	1.6628	2.4024	212.50	131.70	55
8	8	9	5.3434	3.1320	0	0	20
9	9	10	2.1522	1.2615	266.05	164.88	20
10	2	11	0.4052	0.5855	85.00	52.68	70
11	11	12	1.1524	1.6650	340	210.71	70
12	12	13	0.5261	0.7601	297.50	184.37	55
13	13	14	1.2358	1.1332	191.25	118.53	30
14	14	15	2.8835	2.6440	106.25	65.85	20
15	15	16	5.3434	3.1320	255.00	158.03	20
16	3	17	1.2942	1.1867	255.00	158.03	70
17	17	18	0.7027	0.6443	127.50	79.02	55
18	18	19	3.3234	1.9480	297.50	184.37	40
19	19	20	1.5172	0.8893	340	210.71	25
20	20	21	0.7127	1.0296	85.00	52.68	20
21	4	22	8.2528	2.9911	106.25	65.85	20
22	5	23	9.1961	3.3330	55.25	34.24	20
23	6	24	0.7463	1.0783	69.70	43.20	20
24	8	25	2.0112	0.7289	255.00	158.03	20
25	8	26	3.3234	1.9480	63.75	39.51	20
26	26	27	0.5261	0.7601	170	105.36	20

4.3. ESUSCON isolated microgrid

The ESUSCON (Energía Sustentable Cóndor) isolated microgrid is a distribution grid located in the Tarapacá region of Chile, specifically within the Huatacondo area. It represents Chile's first isolated microgrid designed for electricity generation based on non-conventional renewable energies.

The parameters of this microgrid, which comprises a PV plant, a diesel assembly, and an energy storage system, are detailed in Table 5 [17]. It is important to note that this research addresses energy management within the PVDGs to lower operating costs without delving into battery energy management (in an scenario with no energy storage devices), as it is not primarily concerned with battery management. For more information on the ESUSCON microgrid, see [26, 6].

Below, we present the solar generation and energy demand profiles for Huatacondo on a typical day of operation. Such profiles were derived from data from 2018, a year chosen for its abundance and accuracy in the information provided by the Energy Center at the University of Chile. Importantly, the resulting profiles take into consideration the energy variations due to seasonal changes in the Tarapacá region. Considering seasonal variations is essential for evaluating the sustainability and reliability of the system in real-world scenarios. Including these variations ensures that the model accounts for significant fluctuations in solar generation and energy demand, enhancing the robustness of the analysis. This consideration is particularly relevant for solar systems, where irradiance and

Table 5. Parameters for the ESUSCON isolated microgrid.

Parameter	Value	Unit
PV panel power	22.68	[kW]
Maximum storage power	40	[kW]
Storage capacity	150	[kWh]
Maximum generator power	120	[kW]
Minimum generator power	10	[kW]

generation can vary significantly throughout the year. Table 6 reports the duration of each season, and Figures 6 and 7 present the solar generation and energy demand profiles for Huatacondo across the four seasons of the year, respectively.

Table 6. Period of analysis.

Season	Start	End
Summer	21-12-2017	20-03-2018
Autumn	21-03-2018	20-06-2018
Winter	21-06-2018	20-09-2018
Spring	21-09-2018	21-12-2018

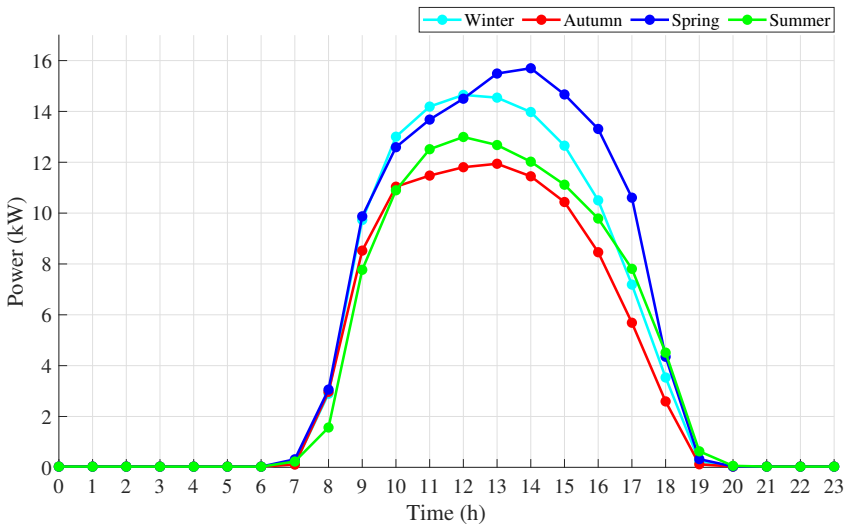

Figure 6. Solar generation profile for Huatacondo (Chile) [6].

The electrical configuration of the system that represents the ESUSCON isolated microgrid is illustrated in Figure 8. This grid operates on a three-phase system, delivering power to devices via a single-phase output point. It operates at a consumption and distribution voltage of 220 V and 380 V, respectively. It is classified as a low-voltage isolated microgrid with overhead lines. The operating frequency within this electrical system is 50 Hz [6]. Additionally, the system's base voltage and power were set at 380 V and 100 kVA, respectively.

Table 7 reports the parameters for the ESUSCON grid, following the format used in Table 3. To establish the maximum current, we calculated an hourly power flow within the system, assuming that there were no PVDGs

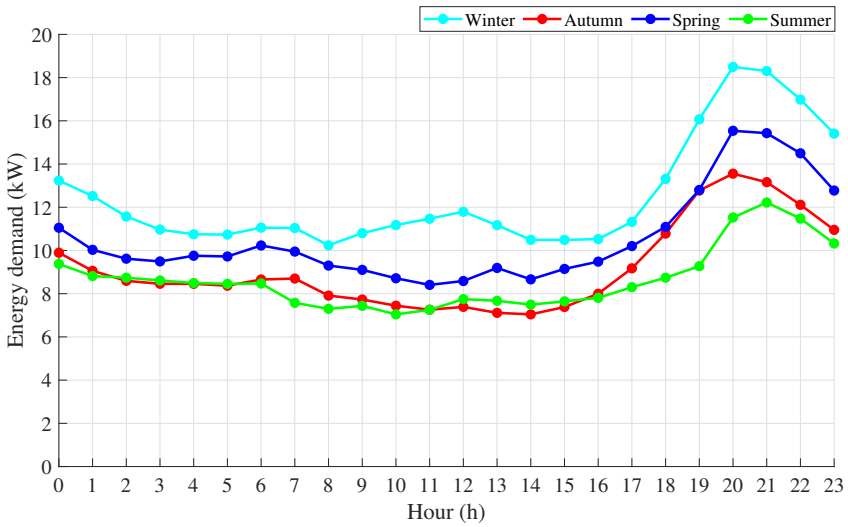

Figure 7. Energy demand profile for Huatacondo (Chile) [6].

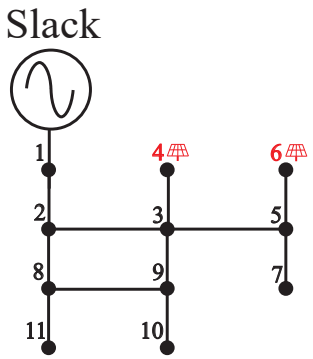

Figure 8. Electrical configuration of the ESUSCON isolated microgrid.

and setting the current thresholds based on the NTC 2050 standard. The conductors were assumed to work at 60°C [25].

5. Results of the simulations

This section reports and discusses the simulation outcomes after implementing the suggested strategies for the intelligent operation of PVDG units within isolated distribution grids. We describe the parameters employed in each optimization method and their results across various test scenarios, encompassing the optimal solution, average solution, standard deviation, difference between the optimal and average solutions, and processing times of each method. Finally, upon identifying the best approach, we evaluated its effectiveness in the ESUSCON isolated microgrid.

Table 7. Electrical parameters for the ESUSCON isolated microgrid.

Line	**Node** i	**Node** j	R_{ij} (Ω)	X_{ij} (Ω)	P_j **[kW]**	Q_j **[kVAr]**	I_{max} **[A]**
1	1	2	0.0339	0.0081	5.1030	1.7213	55
2	2	3	0.0677	0.0085	0	0	40
3	3	4	0.0919	0.0088	0	0	55
4	3	5	0.0677	0.0085	2.5506	0.8603	20
5	5	6	0.0919	0.0088	2.5506	0.8603	20
6	5	7	0.0677	0.0085	1.2762	0.4305	20
7	2	8	0.0677	0.0085	3.1887	1.0756	20
8	8	9	0.0919	0.0088	0	0	20
9	8	11	0.0919	0.0088	1.2762	0.4305	20
10	9	10	0.0919	0.0088	2.5506	0.8603	20

5.1. Optimization parameters

This subsection outlines the parameters employed in each of the four optimization techniques that were implemented in the master stage. As observed, Table 8 specifies the employed optimization method, the parameter subject to tuning, and the value assigned to each parameter. These parameter values were established through heuristic methods.

Table 8. Optimization parameters.

Method	Parameter	Value
MC	Number of individuals	50
	Maximum iterations	2000
GA	Number of individuals	40
	Maximum iterations	4000
	Number of mutations	20
PGA	Number of individuals	100
	Maximum iterations	2000
	Number of mutations	20
	Number of offspring (N)	80
PSO	Number of individuals	50
	Maximum iterations	100
	Velocity limit	0.1
	Maximum inertia	1
	Minimum inertia	0
	Cognitive component	1.494
	Social component	1.494

5.2. Results obtained in the 10-bus test feeder

Table 9 presents the simulation outcomes from assessing the proposed solution methods in the 10-bus test feeder. This table details the employed optimization approach, the optimal (highest reduction) and average solutions, and the average standard deviation. In addition, it delineates the difference between the optimal and average solutions and the average time taken when executing the methodologies 100 times.

Figure 9, for its part, illustrates the impact of the results reported in Table 9. Figure 9 (a), on the one hand, shows the highest reductions achieved by the solution methods in comparison to the base case. Figure 9 (b), on the other

Table 9. Outcomes of the simulations conducted on the 10-bus test feeder.

Method	Best solution [USD]	Average solution [USD]	Average standard deviation [%]	Difference between solutions [%]	Time [s]
MC	49,093.3047	49,645.5337	0.2211	1.1123	391.6731
GA	49,043.2376	49,208.5216	0.1412	0.3359	9.9956
PGA	51,951.6242	52,047.0628	0.0391	0.1834	208.2938
PSO	47,562.2743	47,967.2084	0.4764	0.8442	12.0109
Base case	55.671	- - -	- - -	- - -	- - -

hand, depicts the average reductions. Importantly, the base case involves a total energy cost of USD 55,671.00 during a typical operational day in a scenario without PVDGs, which equates to an annual energy generation cost of USD 20,319,915.00.

As can be seen, all the applied approaches significantly reduced the costs associated with energy generation, with an average value of 11.2417% and 10.6948% for the optimal and average solutions, respectively. In economic terms, the methodologies reduced costs by an average of USD 6,258.00 on a typical day of operation, amounting to USD 2,284,312.00 annually. Remarkably, the PSO approach yielded the most substantial reduction in the objective function, with a maximum reduction of USD 6,578.00 during a typical operational day, equivalent to USD 2,400,000.00 annually.

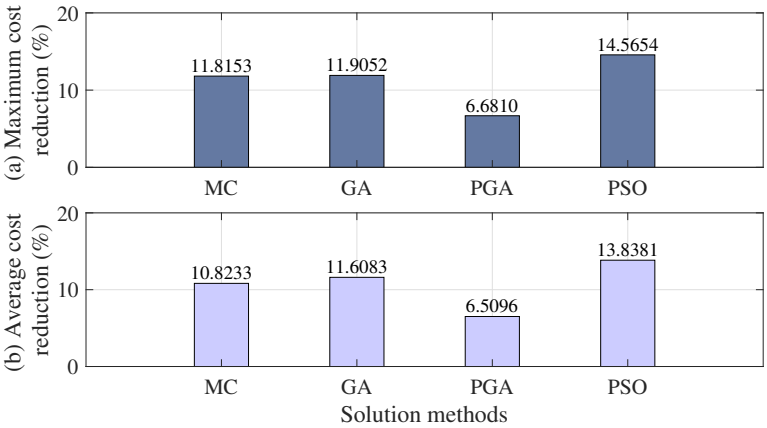

Figure 9. Reductions in power generation costs attained in the 10-bus test feeder.

Regarding the standard deviation obtained by the solution methodologies, running each algorithm 100 times resulted in a maximum and average value of 0.4764% and 0.2211%, respectively (see Table 9). This indicates that the methodology is repeatable, as the maximum standard deviation of 0.48% suggests that similar solutions may be obtained every time the optimization algorithms are executed.

Figure 10 illustrates the impact on solution repeatability and processing times associated with the solution methodologies. Figure 10 (a), on the one hand, depicts the percentage difference between the optimal and average solutions, showing that all approaches exhibited deviations of less than 1.12%. These results demonstrate that, in terms of solution repeatability, all methodologies are suitable. Figure 10 (b), on the other hand, suggests that the processing times of each solution methodology differ significantly, with the CBGA being the most efficient, followed by the PSO, with an approximate difference of two seconds per iteration. The PGA and the MC method were the slowest methods, with a difference of 382 and 198 seconds per iteration, respectively, compared to the other two methods. Despite not being the fastest, the PSO exhibited a slight average increase in processing time

of 2.01536 seconds, achieving optimal results in terms of the objective function. Consequently, in the 10-bus test feeder, the PSO emerges as the most effective technique considering both processing times and solution quality.

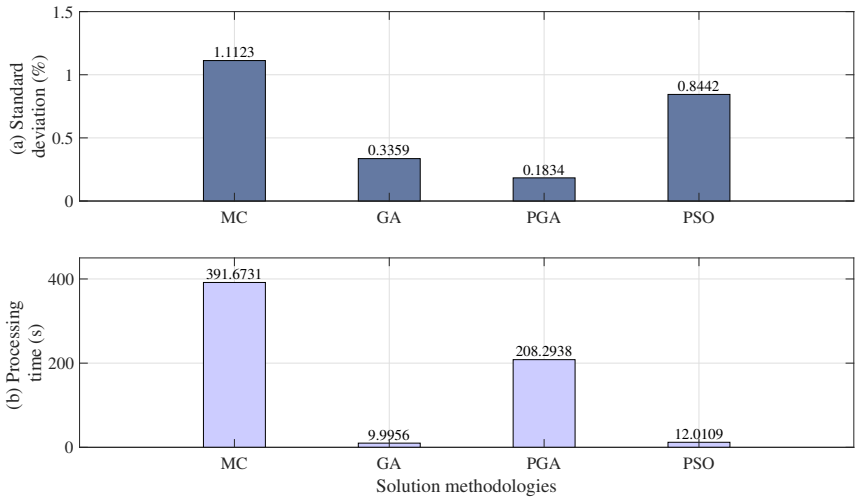

Figure 10. Results obtained in the 10-bus test feeder concerning the standard deviation from the optimal solution and processing time.

The improvements achieved by the PSO in comparison to the other solution approaches are shown in Figure 11. Particularly, Figure 11 (a) depicts the improvements in maximum reductions. As observed, the PSO outperformed the MC method by 3.1186%, the CBGA by 2.5226%, and the PGA by 7.8388%. This translates to an average yearly reduction of USD 364,000.00 concerning the optimal solution. Figure 11 (b), for its part, shows the average improvements achieved by the PSO in comparison to the other techniques, showing an improvement of 11.6212% compared to the MC method, 8.0189% compared to the GA, and 2.9487% compared to the PGA. On average, this reduction equates to USD 373,000.00 annually.

Finally, to verify that the technical requirements of the system are met, we examined the behavior of the voltage profiles and line loadability of the optimal solution obtained from each method, as shown in Figure 12. Figure 12 (a) displays the highest voltage fluctuations at the nodes with respect to the nominal voltage (in p.u.) for each hour of the day. Clearly, all values fall within the range specified by the technical standard, that is, below the threshold of ±8% in voltage variation. Additionally, as observed in Figure 12 (b), the highest line loadability that was achieved using the different solution approaches respects the upper limit. Thus, it is ensured that the solution methods employed to address the PVDG operation problem in the 10-bus test system satisfy the voltage and current constraints.

5.3. Results obtained in the 27-bus test feeder

Table 10 reports the simulation outcomes after assessing the proposed strategies for lowering energy purchase costs in the 27-bus isolated grid. It specifies the applied optimization technique, the optimal (highest reduction) and average solutions, and the average standard deviation. In addition, it delineates the difference between the optimal and average solutions and the average time taken when executing the methodologies 100 times.

Figure 13 illustrates the impact of these results regarding the objective function and problem constraints. Specifically, it shows the reductions achieved by the solution methods in comparison to the base case. This latter entails a total energy cost of USD 18,543 during a typical operational day in a scenario with no PVDGs, which equates to an annual energy purchase cost of USD 6,768,560. Figure 13 (a), on the one hand, depicts the highest reductions when compared to the base case, averaging at 30.7996% for all methodologies. Figure 13 (b), on the other hand, shows the mean reductions, averaging at 29.5244%.

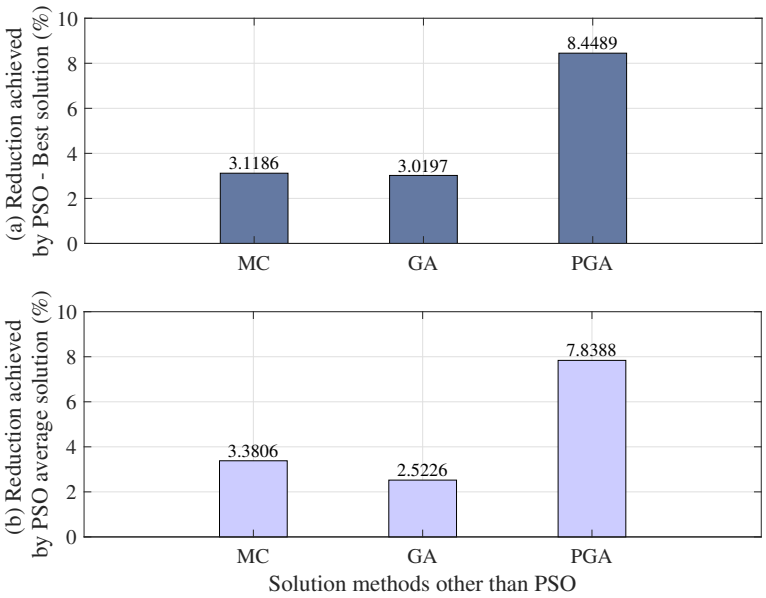

Figure 11. Maximum and average energy generation cost reductions in comparison to the PSO method in the 10-bus test feeder.

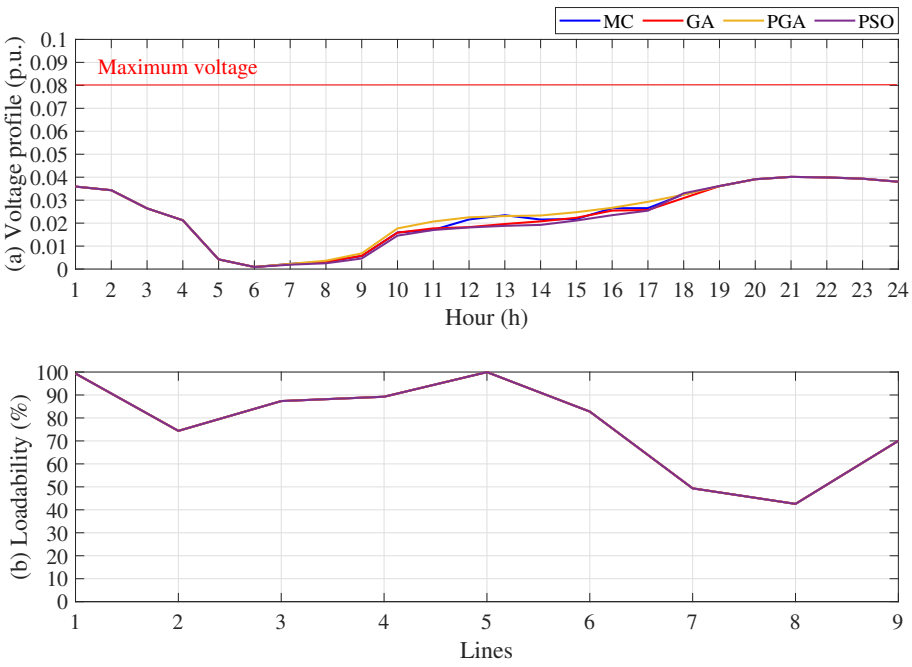

Figure 12. Voltage profile and line loadability of the optimal solution in the 10-bus test feeder.

Table 10. Outcomes of the simulations conducted on the 27-bus test feeder.

Method	Best solution [USD]	Average solution [USD]	Average standard deviation [%]	Difference between solutions [%]	Time [s]
MC	13,508.6263	13,920.5936	0.8878	2.9594	397.0603
GA	13,159.5540	13,375.4074	0.5096	1.6138	9.0854
PGA	12,577.0017	12,676.6478	0.2658	0.7861	534.9691
PSO	12,084.4407	12,302.8502	1.0195	1.7753	10.3640
Base case	18,544	- - -	- - -	- - -	- - -

As observed, all the implemented approaches significantly reduced the costs associated with energy purchase. In economic terms, the methodologies reduced costs by an average of USD 5,711 during a typical operational day, amounting to USD 2,084,784 annually. Remarkably, the PSO provided the optimal solution concerning the objective function, with a maximum reduction of USD 6,459 during a typical operational day, which equates to USD 2,357,681 annually.

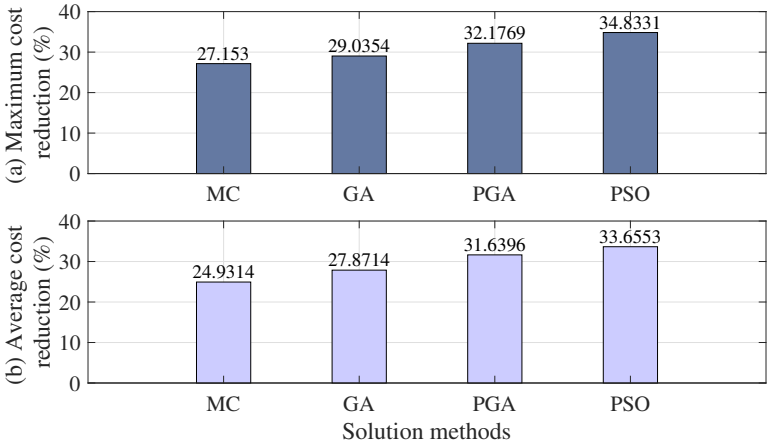

Figure 13. Reductions in power generation costs attained in the 27-bus test feeder.

Figure 14 analyzes solution repeatability and the processing times associated with the solution methods. Concerning the standard deviation obtained by the methodologies, running each algorithm 100 times yielded a maximum and average value of 1.02% and 0.6707%, respectively. Figure 14 (a) displays the standard deviation between the best and average solutions. In terms of solution repeatability, all methodologies produced satisfactory outcomes, with deviations remaining below 3%. Figure 14 (b), for its part, shows the required processing times. As can be seen, similar to the 10-bus grid, there were notable differences in processing times among the methods during the iterations, with the GA being the most efficient, followed by the PSO, with an approximate difference of 1 second per iteration. The PGA and the MC method were the slowest methods, with a difference of 525 and 387 seconds per iteration, respectively, compared to the other two. Although the GA proved to be the fastest, the PSO differs marginally by only 1.2786 seconds, yielding superior results for the objective function. Hence, in the 27-bus test feeder, the PSO emerges as the most efficient technique considering both processing times and solution quality.

The improvements achieved by the PSO in comparison to the other solution approaches are shown in Figure 15. Notably, Figure 15 (a) depicts the improvements in maximum reductions. As observed, the PSO outperformed the MC method by 10.5428%, the GA by 8.1698%, and the PGA by 3.9164%. This translates to an average yearly reduction of USD 364,000.00 concerning the optimal solution. Figure 15 (b), for its part, illustrates the improvements in average reductions achieved by the PSO in comparison to the other techniques, showing an

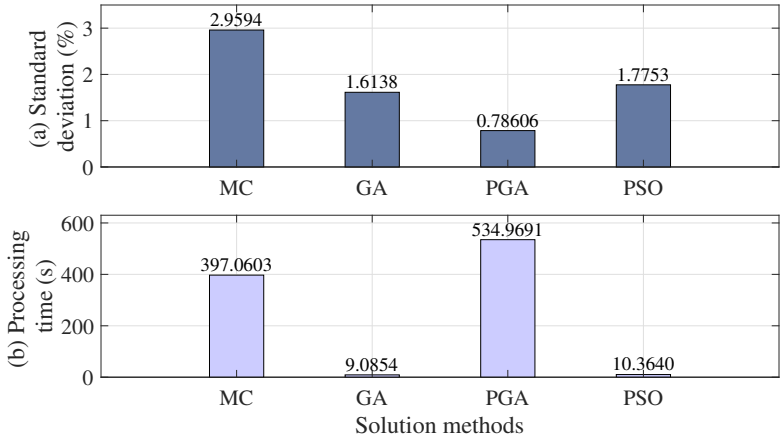

Figure 14. Results obtained in the 27-bus test feeder concerning standard deviation from the optimal solution and processing time.

improvement of 11.6212% compared to the MC method, 8.0189% compared to the GA, and 2.9487% compared to the PGA. On average, this reduction amounts to USD 373,000.00 annually, which is deemed a significant figure.

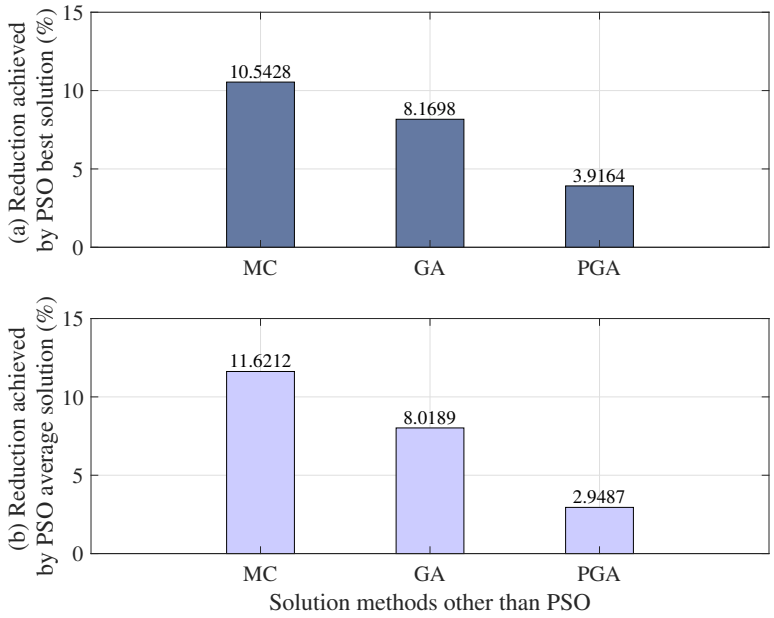

Figure 15. Maximum and average energy generation cost reductions in comparison to the PSO method in the 27-bus test feeder.

Finally, to ensure compliance with regulations regarding technical operational conditions, we examined the behavior of the voltage profiles and line loadability of the optimal solution obtained from each method, as shown in Figure 16. Figure 16 (a) displays the highest voltage fluctuations at the nodes with respect to the nominal voltage (in p.u.) for each hour of the day. Clearly, all values fall within the range specified by the technical standard,

that is, below the threshold of ±8% in voltage variation. Additionally, as observed in Figure 16 (b), the highest line loadability that was achieved using the different solution approaches respects the upper limit. Therefore, it is ensured that the solution methods employed to address the PVDG operation problem in the 27-bus test feeder satisfy the voltage and current constraints.

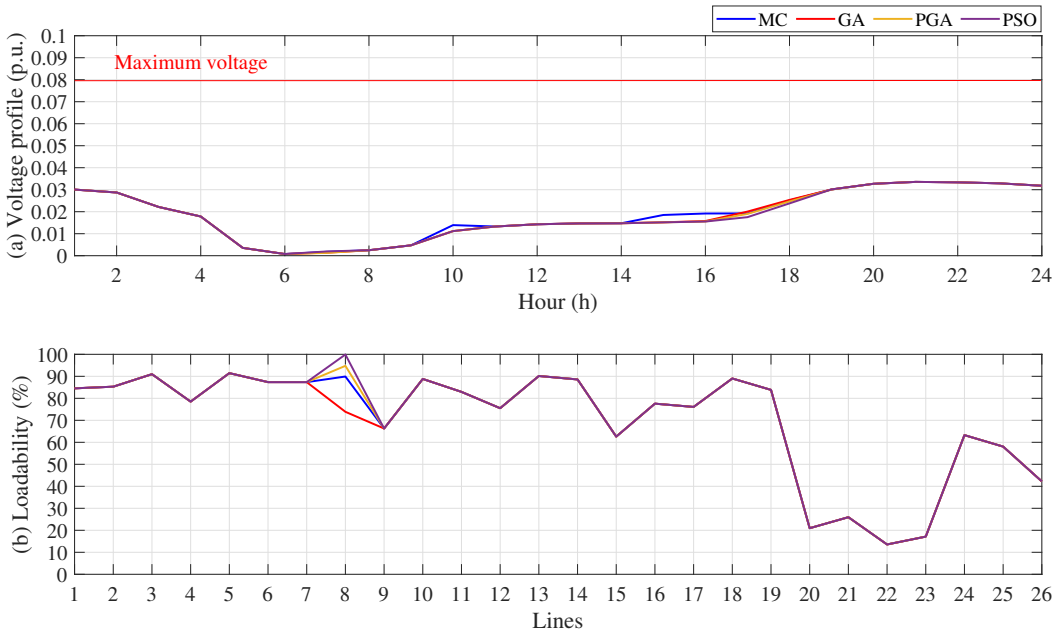

Figure 16. Voltage profile and line loadability of the optimal solution in the 27-bus test feeder.

5.4. *Validation of our solution approach in the Huatacondo microgrid located in the region of Tarapacá in Chile*

This subsection presents and discusses the outcomes derived from implementing and validating the PSO method in an isolated microgrid located in the region of Tarapacá in Chile. Importantly, the robustness and effectiveness of our solution approach were validated using the region's generation and demand curves during a typical operational day across all four seasons of the year: summer, autumn, winter, and spring. With this, we sought to determine the average effects on the costs of operating the grid across the four seasons. The decision to use the PSO as the solution approach was based on the outcomes observed in both the 10-bus and 27-bus test feeders.

Table 11. Reductions achieved by the PSO method (in an scenario with PVDGs) when compared to the base case across all four seasons.

Season	PSO (with PVDGs) [USD]	Time [s]	Base case (with no PVDGs) [USD]
Summer	49.5598	7.6801	67.8690
Autumn	52.6141	13.5662	71.8492
Winter	65.0303	19.1130	98.1352
Spring	57.7766	24.1952	82.6392

Table 11 details the season of the year, the costs of producing energy and maintaining the solar panels when using the PSO approach for the intelligent operation of PVDGs, the method's processing time, and the costs reported in the baseline scenario (with no PVDGs). As observed, in the summer season, the PSO reduced energy usage costs

by USD 18.3092, which corresponds to a reduction of 26.9772%. In autumn, the PSO achieved a cost reduction of USD 19.2351, equivalent to 26.7715%. In winter, the PSO reduced costs by USD 33.1050, which represents a reduction of 33.7340%. Lastly, in spring, the reduction amounted to USD 24.8626, which translates to a percentage decrease of 30.0858%. According to these results, in comparison to the base case, the costs of operating the grid using the PSO methodology with PVDGs were lower in all seasons. This implies that this optimization technique effectively lowered energy generation costs.

Regarding processing times, all were below 24.1952 seconds, with spring exhibiting the lengthiest iteration duration. Consequently, our methodology is deemed efficient in terms of execution times under the evaluated conditions, as it makes it possible to obtain a complete day's operation scheme in less than 25 seconds. This bears significance because the PSO methodology can provide satisfactory results within a reasonable time, making it more practical for real-world applications.

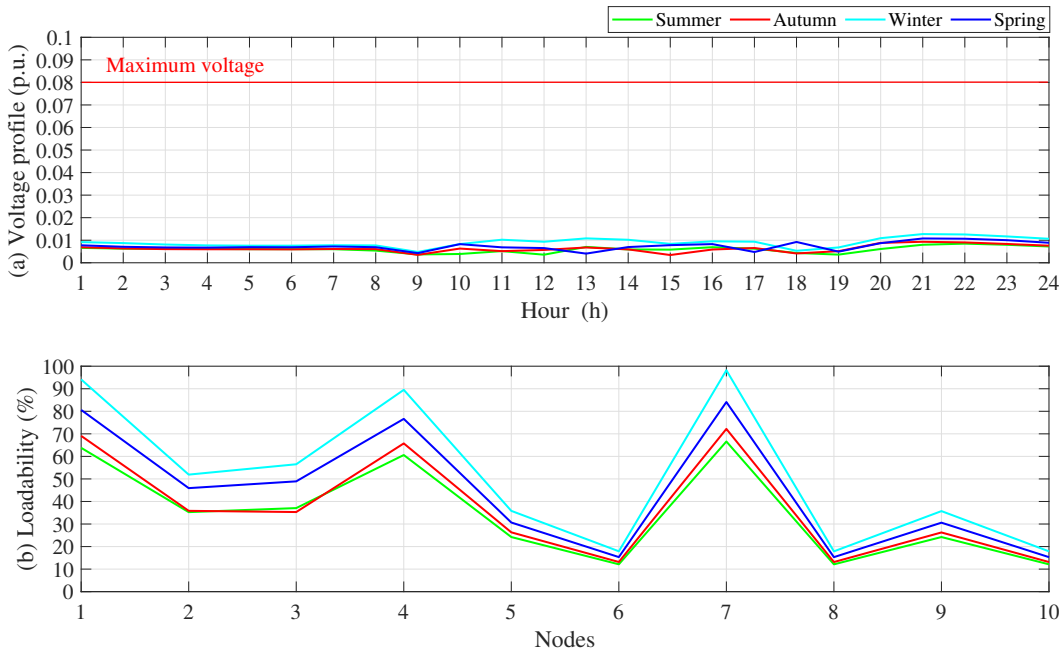

Figure 17. Voltage profile at nodes and line loadability of the PSO methodology implemented in the Huatacondo system.

To verify that the applied methodology satisfied the technical requirements of the Huatacondo grid, we evaluated the voltage profile at nodes and line loadability using the solution generated by the PSO technique. Figure 17 shows the results of this evaluation. Figure 17 (a), on the one hand, depicts the voltage profile at nodes, and Figure 17 (b), on the other hand, illustrates the line loadability. Regarding the voltage profile at nodes, the results confirm that the value provided by the PSO methodology aligns with the permissible range of variation specified in the technical standard. Concerning line loadability, all lines remained below the maximum limit of 100%. These two results demonstrate that the PSO method delivers appropriate solutions in line with the operational requirements of the Huatacondo system, thereby ensuring compliance with regulatory standards.

6. Conclusions

This section summarizes the main findings derived from this study, which concentrated on optimizing the daily operation of PVDGs within isolated AC grids. Particularly, it analyzes the simulation outcomes from the experimental and real-world scenarios considered to evaluate the effectiveness of the proposed solution methods.

In the 10-bus test feeder, the PSO algorithm demonstrated superior performance compared to other approaches in terms of maximum and average reductions in the objective function. In comparison to the other techniques, the PSO showed an average improvement of 4.8624% and 4.5807% in maximum and average operating cost reductions, respectively. Concerning the average standard deviation and the difference between the optimal and average solutions, it yielded a value of 0.4764% and 0.8442%, respectively. This guarantees consistent and accurate solutions with minimal dispersion in each execution of the methodology. Regarding processing times, the PSO method proposed a complete day's operation scheme for the PVDGs integrated into the isolated grid within just 10 seconds, which is deemed efficient for the analyzed scenario. It is worth mentioning that although the GA was two seconds quicker than the PSO, its susceptibility to local optima compromised its efficiency concerning processing time.

In the 27-bus test feeder, once again, the PSO demonstrated superior performance in both maximum and average reductions in the objective function. Upon comparing its results with those of the other methods, the PSO yielded an average improvement of 7.5430% and 7.5296% in maximum and average reductions, respectively. Regarding the standard deviation and the difference between the optimal and average solutions, all methodologies presented values below 1.02% and 2.96%, respectively. This underscores the efficiency of all methodologies in terms of solution repeatability for the 27-bus test feeder. Despite the GA exhibiting the shortest processing time, the PSO yielded satisfactory results with just a 1-second difference in average processing time compared to the GA. These findings suggest that, considering the PSO's superior solution quality and reduced processing times, it emerges as the most efficient approach for addressing the challenge of operating PVDGs within the 27-bus isolated grid.

Given the PSO's superior performance in both test feeders, this study deems it the most appropriate methodology among those we employed to tackle the challenge of the intelligent operation of PVDGs in isolated electrical grids, taking into account fluctuations in energy generation and demand.

Furthermore, to assess the PSO's effectiveness in a real isolated grid amid the varying generation and demand typical of Chile's climatic conditions, we validated the proposed methodology in ESUSCON, an isolated microgrid located in the region of Tarapacá, specifically in the Huatacondo area. Upon analyzing the findings, it was concluded that, on average, our methodology contributed to reducing the microgrid's operating costs by 29.39%, which translates to USD 23.88 on a typical day of operation across all four seasons. Importantly, winter exhibited the most substantial reductions, with a value of 33.73%, equivalent to USD 33.11 on a typical day of operation—a significant figure in terms of the overall costs of intelligently operating the ESUSCON microgrid.

Regarding processing times, the PSO methodology took 16.14 seconds on average to iterate a typical day of operation across all four seasons. Spring, with a total processing time of 24.20 seconds, exhibited the lengthiest processing duration. This underscores the methodology's ability to provide a quick solution to the optimization challenge associated with PVDGs, making it suitable for real-world applications.

In future studies, we recommend exploring the implementation and development of novel optimization techniques to maximize the outcomes achieved by our proposed methodologies. Additionally, the incorporation of alternative renewable energy sources, such as wind power, into the microgrid, alongside the deployment of energy storage systems, should be analyzed to enhance flexibility and reliability. Developing multi-objective optimization models could provide deeper insights into balancing trade-offs between environmental, technical, and economic aspects, particularly in scenarios involving diverse energy sources and operational constraints. Furthermore, investigating the impact of varying weather conditions on the performance of the proposed methodology would contribute to a more robust and adaptive system design. Once the challenges of operating multiple distributed energy resources are addressed, the feasibility of relocating these resources within the grid to optimize its environmental, technical, and economic performance could be examined. Importantly, all these endeavors should consider the technical, topographic, and climatic limitations of the region hosting the isolated electrical grid, ensuring realistic and region-specific solutions.

Acknowledgements

The authors acknowledge the support provided by ANID FONDECyT through project 11240006 entitled *"Smart energy management methods for improving the economic, technical, and environmental indexes of the alternating current microgrids including variable generation and demand profiles"* at the Engineering Faculty of Universidad de Talca, located at the Curicó campus in Chile. Additionally, part of this research has been founded by he Ministry of Science, Technology and Innovation of Colombia (MINCIENCIAS) and the National Fund for Science, Technology and Innovation (Fondo Francisco José de Caldas) through the support received for the realisation of the research internship under the Valorisation Contingent Funding Contract No. 112721-358-2023, Call. 934 of 2023.

References

[1] Laura Sofía Avellaneda-Gomez et al. "Optimal battery operation for the optimization of power distribution networks: An application of the ant lion optimizer". In: *Journal of Energy Storage* 84 (2024), p. 110684.

[2] CGE. *Formulario N°4 del PMGD PFV Nan*. https://www.sec.cl/sitio-web/wp-content/uploads/2021/06/34220.pdf. Documento entregado por la CGE. 2020.

[3] Copec. *Estaciones de Servicio - Copec*. Accedido en septiembre de 2023. 2023. URL: https://ww2.copec.cl/personas/estaciones-de-servicio.

[4] Brandon Cortés-Caicedo et al. "Energy Management System for the Optimal Operation of PV Generators in Distribution Systems Using the Antlion Optimizer: A Colombian Urban and Rural Case Study". In: *Sustainability* 14.23 (2022). ISSN: 2071-1050. DOI: 10.3390/su142316083. URL: https://www.mdpi.com/2071-1050/14/23/16083.

[5] Brandon Cortés-Caicedo et al. "Optimal Location and Sizing of PV Generation Units in Electrical Networks to Reduce the Total Annual Operating Costs: An Application of the Crow Search Algorithm". In: *Mathematics* 10.20 (2022), p. 3774.

[6] Óscar Delfín Dörner Gallardo. "Diseño de una metodología para generación de Benchmark de micro-redes aisladas y su aplicación a la red Esuscon". In: *Repositorio Universidad de Chile* (2022).

[7] Luis Femado Grisales, Bonie Johana Restrepo Cuestas, et al. "Ubicación y dimensionamiento de generación distribuida: Una revisión". In: *Ciencia e Ingeniería Neogranadina* 27.2 (2017), pp. 157–176.

[8] Luis Grisales-Noreña et al. "Metaheuristic Optimization Methods for Optimal Power Flow Analysis in DC Distribution Networks". In: *Transactions on Energy Systems and Engineering Applications* 1 (Dec. 2020), pp. 13–31. DOI: 10.32397/tesea.vol1.n1.2.

[9] Luis F Grisales-Noreña, Oscar Danilo Montoya, and Carlos Andrés Ramos-Paja. "An energy management system for optimal operation of BSS in DC distributed generation environments based on a parallel PSO algorithm". In: *Journal of Energy Storage* 29 (2020), p. 101488.

[10] Luis Fernando Grisales-Noreña, Oscar Danilo Montoya, and Alberto-Jesus Perea-Moreno. "Optimal Integration of Battery Systems in Grid-Connected Networks for Reducing Energy Losses and CO2 Emissions". In: *Mathematics* 11.7 (2023), p. 1604.

[11] Luis Fernando Grisales-Noreña, Oscar Danilo Montoya, and Carlos Andres Ramos-Paja. "Optimal Location and Operation of PV Sources in DC Grids to Reduce Annual Operating Costs While Considering Variable Power Demand and Generation". In: *Mathematics* 10.23 (2022), p. 4512.

[12] Luis Fernando Grisales-Noreña et al. "Optimal Location and Sizing of Distributed Generators and Energy Storage Systems in Microgrids: A Review". In: *Energies* 16.1 (2022), p. 106.

[13] Luis Fernando Grisales-Noreña et al. "Optimal Power Dispatch of PV Generators in AC Distribution Networks by Considering Solar, Environmental, and Power Demand Conditions from Colombia". In: *Mathematics* 11.2 (2023), p. 484.

[14] Luis Fernando Grisales-Noreña et al. “Power flow methods used in AC distribution networks: An analysis of convergence and processing times in radial and meshed grid configurations”. In: *Results in Engineering* 17 (2023), p. 100915.

[15] David Steveen Guzmán-Romero, Brandon Cortés-Caicedo, and Oscar Danilo Montoya. “Development of a MATLAB-GAMS Framework for Solving the Problem Regarding the Optimal Location and Sizing of PV Sources in Distribution Networks”. In: *Resources* 12.3 (2023). ISSN: 2079-9276. DOI: 10.3390/resources12030035. URL: https://www.mdpi.com/2079-9276/12/3/35.

[16] R. Kennedy J. y Eberhart. “Optimización del enjambre de partículas”. In: *Actas de ICNN’95 - Conferencia internacional sobre redes neuronales*. Vol. 4. 1995, 1942–1948 vol.4. DOI: 10.1109/ICNN.1995.488968.

[17] Fernando Lanas Montecinos. “Desarrollo y validación de un modelo de optimización energética para una microrred”. In: *repositorio Universidad de Chile* (2011).

[18] K.F. Man, K.S. Tang, and S. Kwong. “Genetic algorithms: concepts and applications [in engineering design]”. In: *IEEE Transactions on Industrial Electronics* 43.5 (1996), pp. 519–534. DOI: 10.1109/41.538609.

[19] Juan A. Martinez and Gerardo Guerra. “A Parallel Monte Carlo Method for Optimum Allocation of Distributed Generation”. In: *IEEE Transactions on Power Systems* 29.6 (2014), pp. 2926–2933. DOI: 10.1109/TPWRS.2014.2317285.

[20] Gonçalo Mendes, Christos Ioakimidis, and Paulo Ferrão. “On the planning and analysis of Integrated Community Energy Systems: A review and survey of available tools”. In: *Renewable and Sustainable Energy Reviews* 15.9 (2011), pp. 4836–4854. ISSN: 1364-0321. DOI: https://doi.org/10.1016/j.rser.2011.07.067. URL: https://www.sciencedirect.com/science/article/pii/S1364032111003121.

[21] Oscar Danilo Montoya and Walter Gil-González. “On the numerical analysis based on successive approximations for power flow problems in AC distribution systems”. In: *Electric Power Systems Research* 187 (2020), p. 106454. ISSN: 0378-7796. DOI: https://doi.org/10.1016/j.epsr.2020.106454. URL: https://www.sciencedirect.com/science/article/pii/S0378779620302583.

[22] Oscar Danilo Montoya et al. “Optimal location and sizing of PV sources in DC networks for minimizing greenhouse emissions in diesel generators”. In: *Symmetry* 12.2 (2020), p. 322.

[23] M. H. Moradi and M. Abedini. “A Combination of Genetic Algorithm and Particle Swarm Optimization for Optimal Distributed Generation Location and Sizing in Distribution Systems with Fuzzy Optimal Theory”. In: *International Journal of Green Energy* 9.7 (2012), pp. 641–660. DOI: 10.1080/15435075.2011.625590. URL: https://doi.org/10.1080/15435075.2011.625590.

[24] National Renewable Energy Laboratory. “Renewable Electricity Generation and Storage Technologies”. In: *Renewable Energy Futures Study Renewable Electricity Generation and Storage Technologies* 2 (2012).

[25] Instituto Colombiano de Normas Técnicas y Certificación (ICONTEC). “Código eléctrico colombiano NTC 2050”. In: *Bogotá DC* (1998).

[26] OscarDorner-Uch. *GitHub - OscarDorner-UCH/ESUSCON-Isolated-Microgrid-Benchmark*. 2024. URL: https://github.com/OscarDorner-UCH/ESUSCON-Isolated-Microgrid-Benchmark.

[27] Instituto de Planificación y Promoción de Soluciones Energéticas para Zonas No Interconectadas. *Informes Mensuales de Telimetría, Colombia*. Accedido el 21 de Septiembre 2022. 21 de Septiembre 2022. URL: https://ipse.gov.co/cnm/informe-mensuales-telemetria/.

[28] S. Rahman. “Poder verde: ¿Qué es y dónde podemos encontrarlo?” In: *IEEE Power and Energy Magazine* 1 (2003), pp. 30–37. DOI: 10.1109/MPAE.2003.1180358.

[29] Fraunhofer Chile Research. *Vertimiento de Energía en Centrales Eólicas y Solares Fotovoltaicas del Sistema Eléctrico Nacional*. 2022. URL: https://www.fraunhofer.cl/es/publicaciones/white-papers/vertimiento-energia-centrales-eolicas-y-solares-fotovoltaicas%5C-del-sistema-electrico-nacional%20-2022.html.

[30] Andrés Alfonso Rosales-Muñoz et al. "Optimal Power Dispatch of DGs in Radial and Mesh AC Grids: A Hybrid Solution Methodology between the Salps Swarm Algorithm and Successive Approximation Power Flow Method". In: *Sustainability* 14.20 (2022). ISSN: 2071-1050. DOI: 10.3390/su142013408. URL: https://www.mdpi.com/2071-1050/14/20/13408.

[31] Yamille del Valle et al. "Particle Swarm Optimization: Basic Concepts, Variants and Applications in Power Systems". In: *IEEE Transactions on Evolutionary Computation* 12.2 (2008), pp. 171–195. DOI: 10.1109/TEVC.2007.896686.

[32] Panbao Wang, Wei Wang, and Dianguo Xu. "Optimal sizing of distributed generations in DC microgrids with comprehensive consideration of system operation modes and operation targets". In: *IeEe Access* 6 (2018), pp. 31129–31140.

[33] NASA Prediction of Worldwide Energy Resources. *NASA*. Accedido el Fecha de acceso. 21 de Septiembre 2022. URL: https://power.larc.nasa.gov/.